Egypt. J. Chem. **Vol. 68,** No. 07 pp. 33 - 44 (2025)

Egyptian Journal of Chemistry

http://ejchem.journals.ekb.eg/

Metal complexes of substituted benzimidazole to improve the photostability of rigid PVC: Synthesis, spectral, and DFT studies

Mohamed A. El Awady[1], Mostafa M.H. Khalil[1, *], Ayman A. Abdel Aziz[1], Gehad G, Mohamed[2,3], Abdel Naby M. Salem[1]

[1]*Chemistry Department, Faculty of Science, Ain Shams University, Abbassia, 11566, Cairo, Egypt*
[2]*Chemistry Department, Faculty of Science, Cairo University, Gamaa Street, Giza 12613, Egypt*
[3]*Nanoscience Department, Basic and Applied Sciences Institute, Egypt-Japan University of Science and Technology, New Borg El Arab, Alexandria, 21934, Egypt*

Abstract

A series of Co^{2+}, Ni^{2+}, Cu^{2+} and Zn^{2+} coordination compounds of 4-(((1H-benzo[d]imidazol-2-yl)methyl)amino)phenol (BzIm), as new photo stabilizer for vinyl polymers, $[Co(BzIm)(Cl)_2]$ **(1)**, $[Ni(BzIm)(Cl)_2]$ **(2)**, $[Cu(BzIm)(Cl)_2]$ **(3)** and $[Zn(BzIm)(Cl)_2]$ **(4)** have been synthesized, characterized using microanalysis, fourier transform infrared spectroscopy (FTIR), proton nuclear magnetic resonance (^1H NMR), ultraviolet–visible (UV-Vis) spectrophotometry, mass, electron paramagnetic resonance (EPR)TG, magnetic, thermogravimetry differential thermal analysis (TG/DTA) and conductivity. These studies showed that the complexes were formed in which the ligand 4-(((1H-benzo[d]imidazol-2-yl)methyl)amino) phenol coordinated to the metal ion through benzimidazole nitrogen and the amino group of methylaminophenol. A PVC film containing the novel complexes was synthesized and used as a photo stabilizer for PVC. The results reveal the higher stabilizing potency of some of the substituted benzimidazole metal complexes compared to commercially known reference stabilizers. Based on weight loss as a criterion for photo-stabilizing efficiency the best stabilizing efficiency of the investigated complexes was given by the $[Zn(BzIm)Cl_2]$ (**4**), as after 8h. irradiation, its weight loss is only 2.6 % that of the blank and 3 % that of the the reference stabilizer (Tinuvin P). Additionally, the data of discoloration level of photo-degraded rigid PVC films in presence of the examined complexes stabilizers after 8h of irradiation time is light yellow in case of $[Zn(BzIm)Cl_2]$ (**4**), which is the palest colour relative to other investigated compounds. The photo stabilization efficiency results, based on different parameters including percent weight loss, percent gelation %, stabilizing efficiency were found to be in the following order: $[Zn(BzIm)Cl_2]$ (**4**) > Tinuvin P (**TP**) > $[Ni(BzIm)Cl_2]$ (**2**) > $[Cu(BzIm)Cl_2]$ (**3**) > $[Co(BzIm)Cl_2]$ (**1**). The stabilizing efficiency of these derivatives is attributed to their radical trapping potency which intervenes with the radical degradation process of PVC. The experimental data were more insighted using theoretical calculation using at DFT/B3LYP level of theory, which indicated that Zn(II) Complex (**4**) had the lowest HOMO-LUMO energy gap (1.162 eV) among the complexes under investigation, whereas Co(II) Complex (1) displayed the biggest energy gap (1.307 eV).

Keywords: Photo-stabilizer; Benzimidazole; PVC; DFT; Metal complexes

1. Introduction

One of the most extensively utilized polymers in the world is polyvinyl chloride (PVC), due to its cost-effectiveness, great intrinsic qualities, and adaptability[1, 2]. In polymer chemistry photo-oxidation (sometimes: oxidative photodegradation) is the degradation of a polymer surface due to the combined action of light and oxygen. It is the most significant factor in the weathering of plastics. Photo-oxidative degradation is a result of light-induced reactions in polymers that lead to color changes, chalking, cracking, and a reduction in mechanical qualities like elongation, tensile strength, and impact strength, etc. [3, 4]. Additives can retard the photo-degradation of polymers in two primary ways: UV Absorption and Scavenging: Some additives, like UV stabilizers, absorb harmful ultraviolet (UV) radiation, preventing it from penetrating the polymer and initiating degradation processes. By converting UV energy into harmless heat or by scavenging free radicals generated by UV exposure, these additives help maintain the integrity of the polymer [5]. The following stabilizing systems have been developed, which depend on the action of stabilizer: (1) light screeners, (2) UV absorbers, (3) excited-state quenchers, (4) peroxide decomposers, and (5) radical scavengers. Certain additives, such as antioxidants or fillers, can form a protective barrier that reduces the polymer's exposure to oxygen and light. This barrier can slow down the oxidative reactions that lead to degradation, thereby

---

*Corresponding author e-mail: khalil62@yahoo.com.; (Mostafa M. H. Khalil).

Receive Date: 02 October 2024, **Revise Date:** 03 November 2024, **Accept Date:** 06 November 2024
DOI: https://doi.org/10.21608/ejchem.2024.325414.10570

extending the material's lifespan in outdoor applications [5]. Together, these mechanisms help enhance the durability and longevity of polymer materials under light exposure.

Imidazole and benzimidazole, along with their derivatives, hold significance in various fields such as coordination chemistry, photophysics, photochemistry, and bioinorganic chemistry. These compounds exhibit diverse properties and applications due to their unique structures and reactivities. In coordination chemistry, they often serve as ligands that can coordinate with metal ions to form coordination complexes with specific properties and applications. In photophysics and photochemistry, these compounds are of interest due to their light-absorbing and emitting properties, which can be utilized in various applications such as sensors, light-emitting diodes, and photodynamic therapy. In bioinorganic chemistry, imidazole and benzimidazole derivatives are important due to their interactions with metal ions in biological systems, which play crucial roles in processes such as enzyme catalysis and metal ion transport.[6, 7].

Many metal benzimidazole complexes including Cr, Mn, Fe, Co, Ni, Zn, Pd, Pt, Au, and Re have been reported [8-11]. Ryokichi *et al.*, [12] reported square planar to the octahedral transformation of (bzim), nickel(II) nitrate 2.5EtOH. The thermal behavior of coordination compounds of bzim with $Co(NO_3)_2$, $Ni(NO_3)_2$, and $Cu(NO_3)_2$ were studied by Curini *et al.* [13]. Dulova and Petrash studied the electrical conductance and spectral behavior of complexes of benzimidazole with Co(II) and Ni(II) nitrates, and stability constants were calculated for 1:1 and 2:1 metal complexes [14]. Synthesis and the characterization of benzimidazole complexes of Co(II), Ni(II), and Cu(II) were investigated [15], and the complexes of formula $ML_nX_n\ nH_2O$ (M= Co, Ni, Cu; X= Cl^-, SO_4^{2-}, OAc^-) were proposed to have of tetrahedral configuration.

The stability constants of coordination compounds involving cobalt (Co), nickel (Ni), manganese (Mn), and cadmium (Cd) with benzimidazole (bzim) can be determined through potentiometric and spectral methods [16, 17]. UV spectra of benzimidazole, and its derivatives, during protonation and complexation with chlorides of Co(II), Cu(II), and Sn(II) were reported [18]. In $CoCl_2$ and $CuCl_2$ complexes, an σ-dative interaction occurs due to a partial delocalization of metal's d-electrons to antibonding π-orbitals of ligand. The present study aims to synthesize and investigate a new benzimidazole-containing compound (Figure 1), and its complexes that may be used as photo-stabilizers for rigid PVC.

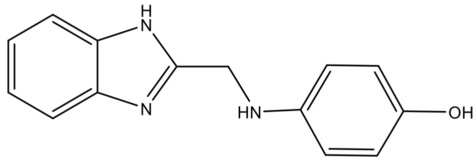

Figure 1. Structure of 4-(((1H-benzo[d]imidazol-2-yl)methyl)amino)phenol (BzIm).

2. Experimental

2.1 Synthesis of benzimidazole ligand (BzIm)

2-Chloromethyl benzimidazole and *p*-aminophenol were condensed in equimolar amount in ethanol with small amount of sodium iodide under stirring for 24h (TLC monitoring). The reaction was cooled, neutralized, filtered, and collected to re-crystallize from ethanol [11, 18, 19].

BzIm ($C_{14}H_{13}N_3O$), Color: brown. MS: M+ = 236 (calcd.239). FT-IR (KBr, cm^{-1}): 3432 $\nu(NH)_{sec}$, 1504 ν(C=N), 1063 ν(N-N), 2887 $\nu(C\text{-}H)_{Ar}$, 1339 ν(C-N). ^{1}H-NMR (DMSO): 13.00 (1H, s, benzimidazole NH); 7.70, 7.54, 7.30 and 7.25 (4H, m, benzimidazole ring (Bz)); 7.39, 7.36, 6.88 and 6.85 (4H, dd, aniline ring (An), 5.00 (1H, t, NH_{sec}), and 4.33 (2H, d, CH_2). UV-Vis (ethanol): 204, 226, 275, 281 and 358 nm. Analysis of the ligand don't show OH phenol signal at room temperature due to intermolecular exchange of the –OH protons with protons of the protic solvents or with protons of the residual H_2O in aprotic solvents [20].

2.2 Synthesis of benzimidazole ligand (BzIm) complexes

Hot ethanolic solution of 4-(((1H-benzo[d]imidazol-2-yl)methyl)amino)phenol, (1 mmol, 239 mg, 20 mL) was added to 1 mmol ethanolic solution of $CoCl_2.6H_2O$ (237.93 mg), $NiCl_2.6H_2O$ (237.71 mg), $CuCl_2.2H_2O$ (170.48 mg) or $ZnCl_2.4H_2O$ (208.34 mg) under stirring for 1-2h to get a precipitate of BzIm complexes.

- **Complex (1)**, $C_{14}H_{13}CoN_3Cl_2O$: Yield: 78% MS: M+ = 369.31 (calcd. 369 g/mol). Elemental analysis (%): calcd.: C 45.65, H 3.55, N 11.38, found C 45.30, H 3.30, N 11.28. FT-IR (cm^{-1}): 3225 $\nu(NH)_{sec}$, 3407ν(OH), 1615 ν(C=N), 435 ν(N-Cl). UV-Vis. (DMF, 10^{-4}, nm): 210, 255 and 270. Λ_m (10^{-3} M, DMF, $\Omega^{-1}cm^2mol^{-1}$): 15.40. μ_{eff} (μ_B, 298 K): 4.07 BM.

- **Complex (2),** $C_{14}H_{13}NiN_3Cl_2O$: Yield: 80%. MS: M+ = 368.40 (calcd. 368.87 g/mol). Elemental analysis (%): calcd.: C 45.58, H 3.55, N 11.39, found C 45.54, H 3.78, N 11.63. FT-IR (cm^{-1}): 3227 $\nu(NH)_{sec}$, 3431ν(OH), 1560 ν(C=N), 433 ν(N-Cl). UV-Vis. (DMF, 10^{-4}, nm): 225, 240, 250, 265 and 290. Λ_m (10^{-3} M, DMF, $\Omega^{-1}cm^2mol^{-1}$): 14.70. μ_{eff} (μ_B, 298 K): 3.20 BM.

- **Complex (3),** $C_{14}H_{13}CuN_3Cl_2O$: Yield: 82%. MS: M+ = 374 (calcd. 373.72 g/mol). Elemental analysis (%): calcd.: C 45.78, H 4.56, N 10.01, found C 44.13, H 3.61, N 10.90. FT-IR (cm^{-1}): 3227 $\nu(NH)_{sec}$, 3430 ν(OH), 1615 ν(C=N), 435 ν(N-Cl). UV-Vis. (DMF, 10^{-4}, nm): 230, 240, 255 and 370. Λ_m (10^{-3} M, DMF, $\Omega^{-1}cm^2mol^{-1}$): 12. μ_{eff} (μ_B, 298 K): 2.05 BM.

- **Complex (4)**, $C_{14}H_{13}ZnN_3Cl_2O$: Yield: 80%. MS: M+ = 376.31 (calcd. 375.56 g/mol). Elemental analysis (%): calcd.: C 44.77, H 3.39, N 11.19, found C 44.78, H 3.46, N 11.90. FT-IR (cm^{-1}): 3243 ν(NH)$_{sec}$, 3429 ν(OH), 1613 ν(C=N), 437 ν(N-Cl). ^{1}H-NMR (DMSO-d_6, δ, ppm): 10.32 (s, 1H, H17), 8.05 (d, 1H, H6), 8.03 (t, 1H, H7), 7.99 (t, 1H, H8), 7.69 (d, 1H, H9), 7.54 (s, 1H, H15), 7. 24 (d, 1H, H13), 7.12 (d, 1H, H12), 2.31 (s, 3H, H16). UV-Vis. (DMF, 10^{-4}, nm): 210, 230, 255 and 375. Λ_m (10^{-3} M, DMF, $\Omega^{-1}cm^2mol^{-1}$): 7.75.

2.3 Materials and Physical Measurements

The materials, methods, and equipment utilized for characterizing the samples and assessing their physical properties are thoroughly described in the supplementary file.

2.4 Preparation of PVC Polymeric Film Samples and Photo-Degradation Study

The methods of preparing homogenous films of PVC additive-free and PVC loaded with complexes as well as the photodegradation study, are described in the supplementary file.

2.5. Computational details

Computational calculations on the ligand and its metal complexes were completed in Gaussian 09 [21]. Various graphic views of molecular charges and shapes of distinctive molecular orbitals were studied by Gauss View 5.0 package.

3. Results and discussion

3.1. Electronic structure, frontier molecular orbitals, and magnetic susceptibility

Five absorption bands appeared at electronic spectra BzIm ligand in ethanol. Two of them lies at 204 and 226 nm which may be attributed to phenyl rings that have medium and low energy π-π* transitions in phenyl of phenol and benzimidazole moiety, respectively [22]. The possible transitions in benzimidazole ring are three types n-π*, π-π*, and charge-transfer. Although benzimidazole system has a lone pair of electrons on the tertiary nitrogen atom, this system has not n-π* transition [23]. So, BzIm bands at 275, 281, and 358 nm may be attributed to benzimidazole ring π-π* transitions. Also, the appeared doublet bands have the lowest energy in the studied compounds which attributed to a tautomeric structure of these derivatives [24].

UV-Vis spectra of the four benzimidazole complexes at 10^{-4} M were scanned in DMF in the region 200-900 nm (Figure S1). The electronic spectrum of the cobalt(II) complex exhibits sharp peaks at 210 and 255 nm with shoulder at 270 nm are assigned to internal ligand transitions ($\pi-\pi^*$) in the benzimidazole ring), and a broad band around 300-350 nm, suggesting that a four-coordinate square planar structure for the studied complexes. The broadness of the band may be taken as an indication of distortion from planar symmetry [25, 26]. The electronic spectrum of nickel (II) complex shows absorption bands at 225, 240, 250, 265, and 290 nm, assigned to $^1A_{2g}\rightarrow{}^1A_{1g}$ transition which are characteristic to square-planar geometry [27, 28]. The Cu(II) complex in its spectrum displays a band centered at 230, 240, 255 and 370 nm, indicating the complex to have distorted square planer geometry [28-30]. Finally, the electronic spectrum of the zinc (II) complex shows absorption bands at 210, 230, 255 and 375 nm, which is attributed to the charge transfer transition, supporting coordination of the zinc(II) ion via nitrogen atom, which is compatible with the complexes with a distorted square planar structure [31], the electronic spectra of these complexes do not show any d-d transition bands.

The complexes of Cobalt, Nickel, and cupper have a magnetic moment of 2.05, 3.20, and 4.07 BM, which may be imputed to one, two and three unpaired electrons, respectively that is compatible with presence of weak filed square planer geometry of these complexes [25, 32]. As expected for d^{10} ions, zinc(II) complex has been found to be diamagnetic in nature.

Vibrational analysis

The presence of broad absorption band at 2200-3500 cm^{-1} which is related to NH group of benzimidazole in its IR spectra as a result of strong hydrogen intermolecular bond between pyridine-type nitrogen, and the benzimidazolic NH group. There are two absorption bands in IR spectrum, the first one at 3513 cm^{-1} which attributed to BzIm NH and the other at 3445 cm^{-1} that indicates presence of free secondary amino group in the compounds.

The presence of a broad absorption band at 2200–3500 cm^{-1}, which is related to the NH group of benzimidazole, in its IR spectra, is a result of a strong hydrogen intermolecular bond between pyridine-type nitrogen and the benzimidazolic NH group. There are two absorption bands in the IR spectrum, the first one at 3513 cm^{-1}, which is attributed to BzIm NH, and the other at 3445 cm^{-1}, which indicates the presence of free secondary amino groups in the compounds.

The infrared spectra of complexes **1-4** (Figure S2), indicate the presence of sharper υ (NH)$_{Bz}$ bands at 3225, 3227, 3227, and 3243 cm^{-1}, respectively, than found in the uncoordinated ligand [33, 34] as a result of breaking of the intermolecular hydrogen bond. Also, C=N group appears at 1682 cm^{-1} in BzIm ligand with low shifting by 12-73 cm^{-1} in the complexes to confirm pyridine-type nitrogen participation in the coordination sphere.

The IR spectrum of BzIm ligand displays a band at 3550-3200 cm^{-1} assigned to the stretching mode of the OH group. Experimentally, this band is assigned to wave numbers (3431-3407 cm^{-1}) in complexes, supporting that this group remains intact in the complex formation. In the far IR spectra of all the complexes, the new bands observed at 433-437 cm^{-1} region can be assigned to Metal-N stretch [35].

^{1}H-NMR

The ^{1}H NMR of the ligand has NH as a clear singlet at 13.00 ppm, while the secondary amino group appeared as triplet at 5.00 ppm and the methine group (CH_2) appeared as a doublet at 4.33 ppm. The protons of aromatics afforded in the region 6.85-7.39 ppm for secondary amino group and at 7.25-7.70 of benzimidazole aromatic protons.

The ^1H NMR of the ligand has NH as a clear singlet at 13.00 ppm [36], while the secondary amino group appeared as a triplet at 5.00 ppm and the methine group (CH_2) appeared as a doublet at 4.33 ppm. The protons of aromatics are afforded in the region 6.85-7.39 ppm with respect to the secondary amino group and at 7.25-7.70 of benzimidazole aromatic protons.

The Zn-complex was examined to confirm the proposed structural formula of the metal chelate (Figure S3). The NH_{sec} group is responsible for the triplet signal in the free ligand, which travels downfield because of its involvement in the chelation, whereas the methylene group, which is present in the complex at 5.56 ppm, is responsible for the triplet signal at 5.00 ppm. Additionally, it is discovered that, in comparison to the other aromatic protons, the aromatic protons closest to the coordination centre's experience the greatest downfield changes.

Thermogravimetric Analysis

The thermal decomposition of $[Co(BzIm)Cl_2]$ (**1**) (Figure S4) occurs through two endothermic steps maximized at 317 and 713 °C, with a mass loss amounting to 75.58% (calcd. 73.19%) assuming (CoO+2C) as a final residue. $[Ni(BzIm)Cl_2]$ (**2**) decomposed through three endothermic stages maximized at 271, 756 and 870 °C, with overall mass loss amounting to 67.28% (calcd. 66.77%), assuming (NiO+4C) as a final residue, The TGA curve of $[Cu(BzIm)Cl_2]$ (**3**), exhibits two decomposition steps at 220 and 457°C, with overall mass loss amounting to 85.66% (calcd. 84.86%) leaving copper metal as a final residue. Thermal degradation of $[ZnBzIm)Cl_2]$ (**4**) proceeds *via* two main steps at 308 and 703 °C, with overall mass loss amounts to 62.44% (calcd. 62.35%), assuming (ZnO+5C) as a final residue.

Mass spectrometry

The electron impact mass spectra of the BzIm complexes were recorded and investigated at 70 eV of electron energy (Figure S5). The fragmentation of the parent molecular ion peaks is given in (Schemes 1). The mass spectrum of $[Co(BzIm)Cl_2]$ (**1**) complex is *m/z* 369 as molecular ion peak which loses OH group and 2 Cl atoms from M^+ to give a fragment ion at *m/z* 282 (Scheme 1). It was found that the involvement of $C=N_{py}$ in chelation introduces a weakness point through which the benzimidazole ring decomposes to imidazole moiety with a fragment at m/z 177, [(imidazole) $CoCl_2$][37].

The strong molecular ion peak of $[Ni(BzIm)Cl_2]$ (**2**) complex is at *m/z* 368.87 with one fragmentation route that is traced by a peak at *m/z* 281.97 owing to the elimination of (OH group) and 2Cl atoms. Further fragmentation occurs by the dissociation of the imidazolic group to provide a fragment at *m/z* 368.87 (Scheme 1).

Also, the molecular ion peak of $[Cu(BzIm)Cl_2]$ (**3**) complex was observed at *m/z* 373.72, which loses two moles of Cl and OH giving an ion at *m/z* 286.82 (Scheme 1).

The mass spectrum of $[Zn(BzIm)Cl_2]$ (**4**) complex has a molecular ion peak at *m/z* 375.56, the spectrum showed peaks at m/z 288.65 owing to the elimination of 2Cl and OH (Scheme 1).

X-ray powder diffraction

XRD patterns of the title complexes (Figure S6), were identified according literature [38, 39], revealed that the pronounced effect of the metal type on the crystallinity of these compounds. Comparing between XRD spectra the free ligand and complexes indicated the amorphous structure of the chelates under study. XRD spectra for chelates showed that the coordination of free ligand and the metal ions changes patterns of XRD in the BzIm ligand. The interstice 3.549 **Å** at $\mathbf{2\theta}$ =25.065 is the interlayer spacing of BzIm-metal complexes, suggesting that all complexes have the same phase structure.

Electron spin resonance spectra (ESR)

The distribution of the unpaired electrons and the bonding nature between ligand and metal ion are clarified via electron spin resonance spectra. These studies showed a paramagnetic transition metal(II) complex. the powdered X-band ESR spectrum of the complex Cu(II)-BzIm complex at room temperature is shown in Figure S7. The ESR spectrum of the copper complex is of the axial type $g_{II} > g_I > 2.0023$ and is consistent with a species having a square structure [40, 41].

Photo stabilization of PVC

a. Weight loss as a criterion for photo-stabilizing efficiency

Weight loss follows the well-known dehydrochlorination process (the evolution of HCl gas) that is typically associated with photo-degradation of PVC. This phenomenon is known to intensify with an increase in irradiation time. As a result, the weight loss % as a function of irradiation time may be used to estimate the degree of degradation and, in turn, the stabilizer's stabilizing potency and duration of polymer protection. Table 1 presents the weight loss (%) of BzIm complexes as a function of photo-irradiation time (Figure 2a). The results revealed the low extent of weight loss of photodegraded PVC stabilized with all the investigated BzIm complexes as compared with the blank PVC sample. $[Zn (BzIm)Cl_2]$ (**4**) complex as compared with the unmodified reference UV-stabilizer Tinuvin P (**TP**), while $[Co (BzIm)Cl_2]$ (**1**), $[Ni(BzIm)Cl_2]$ (**2**) and $[Cu(BzIm)Cl_2]$ (**3**) complexes gave a slightly higher weight loss % as compared with the reference Tinuvin P. On the other hand, the best stabilizing efficiency of the investigated complexes was given by the $[Zn(BzIm)Cl_2]$ (**4**), as after 8h. irradiation, its weight loss is only 2.6 % that of the blank and 3 % that of the reference stabilizer. The stabilizing efficiency of the investigated photo-stabilizers was found to follow the following order: $[Zn(BzIm)Cl_2]$ (**4**) > Tinuvin P (**TP**) > $[Ni(BzIm)Cl_2]$ (**2**) > $[Cu(BzIm)Cl_2]$ (**3**) > $[Co (BzIm)Cl_2]$ (**1**).

.

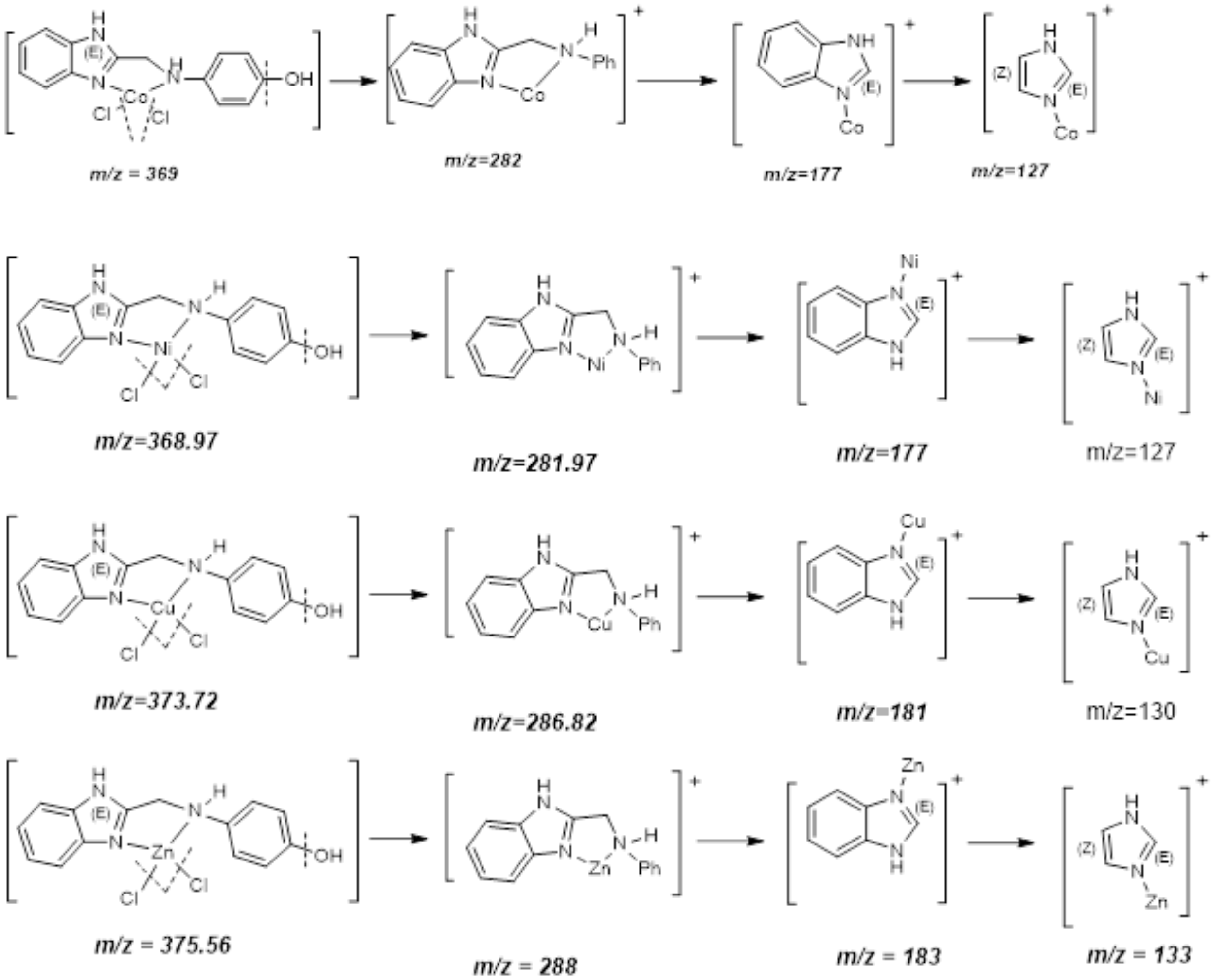

Scheme (1): Fragmentation pattern of BzIm Complexes

b. Amount of gel as criterion for photo-stabilizing efficiency

The percent of gelation of photodegraded PVC (blank or stabilized) with the reference stabilizer (Tinuvin P) are documented in Table 1 and Figure 4a. The stabilizing efficiency as determined by the amount of gel formation correlates well with the results obtained from the % weight loss dat. So, the order: [Zn(BzIm)Cl_2] (**4**) > Tinuvin P (**TP**) > [Ni(BzIm)Cl_2] (**2**) > [Cu(BzIm)Cl_2] (**3**) > [Co(BzIm)Cl_2] (**1**).

c. Soluble fraction as criterion for photo-stabilizing efficiency

The % soluble fraction of either photo-degraded blank PVC or stabilized photo-degraded PVC or photo-degraded blank PVC, or for photo-degraded PVC with metal-BzIm complexes (as a function of irradiation time) are agreed well with the % gelation (Table 1 and Figure 2c). this is another proof for the results obtained for gel formation.

d. Extent of discoloration as criterion for photo-stabilizing efficiency

The level of discoloration of photo-degraded films of rigid PVC, in presence of the examined complexes stabilizers as a function of irradiation time is depicted in Table 2. Additionally provided for comparison is the degree of discoloration of the PVC blank and the PVC sample stabilized by the reference Tinuvin-P photo-stabilizer. The data revealed the low extent of discoloration of all the investigated PVC samples stabilized by the complex stabilizers as compared with the blank sample. The stabilizing efficiency of the investigated compounds was found to be in the following order: [Zn(BzIm)Cl_2] (**4**) > Tinuvin P (**TP**) > [Ni(BzIm)Cl_2] (**2**) > [Cu(BzIm)Cl_2] (**3**) > [Co(BzIm)Cl_2] (**1**).

Molecular DFT calculation

Compounds' three-dimensional shapes can be explained by molecular geometries discovered theoretically. At the DFT level of B3LYP/6-311++G (d, p), all compounds were optimized [20]. Figure 3 displays the optimized geometries of the ligand under investigation (BzIm) and its complexes **1-4**.

The HOMO and LUMO frontier molecular orbitals (FMOs) are essential for predicting a molecule's reactivity and anti-free radical action [42, 43]. The primary players in electronic transitions are the anti-free radical's lowest unoccupied molecular orbital (LUMO) and highest occupied Frontier molecular orbital (HOMO) energies; their energy gap represents the reactivity [44]. At the B3LYP/6-311++G (d, p) level of DFT, the ligand's HOMO and LUMO, as well as those of its complexes 1-4, were investigated. Figure 4 displays the distribution pattern of the ligand's and its complexes' frontier molecular orbitals (HOMOs and LUMOs) at the ground states, along with the related energies. Table lists the specific HOMO and LUMO energies of compounds 1-4 along with their gaps.

Zn(II) Complex (**4**) had the lowest HOMO-LUMO energy gap (1.162 eV) among the complexes under investigation, whereas Co(II) Complex (1) displayed the biggest energy gap (1.307 eV). In addition, the difference between the LUMO and HOMO energies (ΔE = ELUMO - EHOMO) is crucial for predicting a compound's chemical response. One further crucial element in determining a compound's activity is the energy differential between its LUMO and HOMO. A small energy gap shows the compound's softness (reactivity), whereas a big gap suggests its hardness (stability).

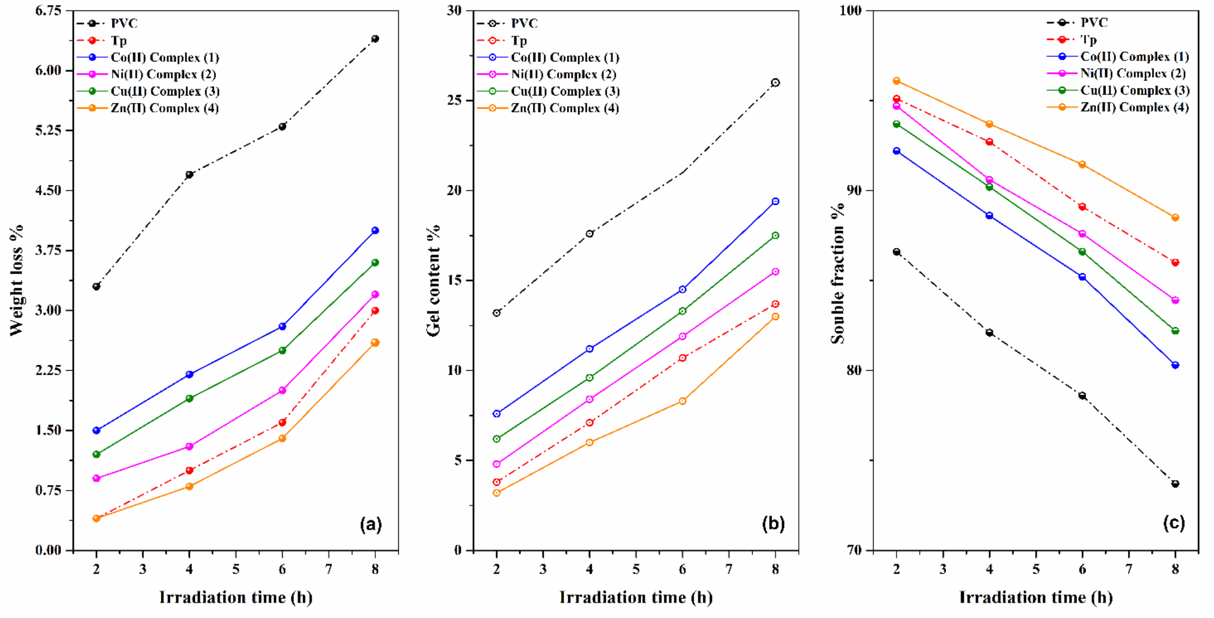

Figure 2. Variation of weight loss (%), gel content (%) and soluble fraction of M(II)-BzIm complexes with irradiation time (h).

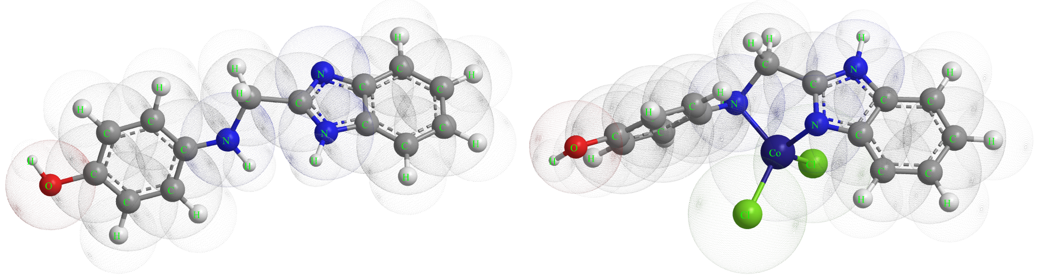

BzIm

[Co(BzIm)Cl_2] (**1**) complex

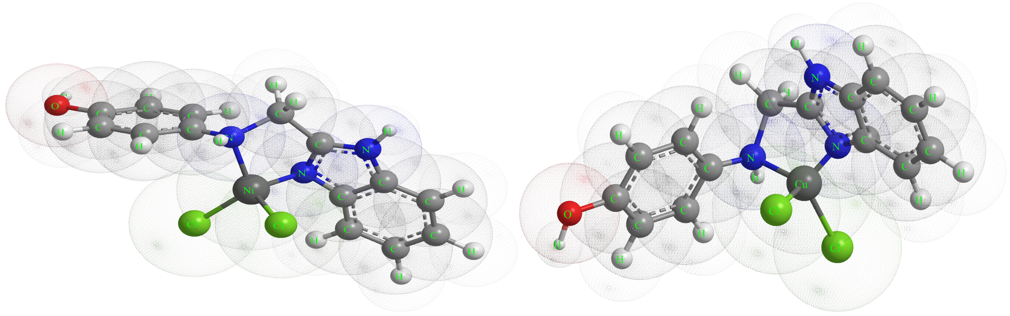

[Ni(BzIm)Cl_2] (**2**) complex

[Cu(BzIm)Cl_2] (**3**) complex

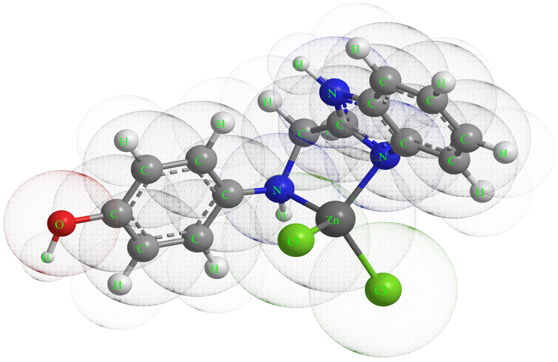

[Zn(BzIm)Cl_2] (**4**) complex

Figure 3. The optimized geometries of the ligand (BzIm) and its complexes (**1-4**) at the B3LYP/6-311++G (d, p) level of DFT.

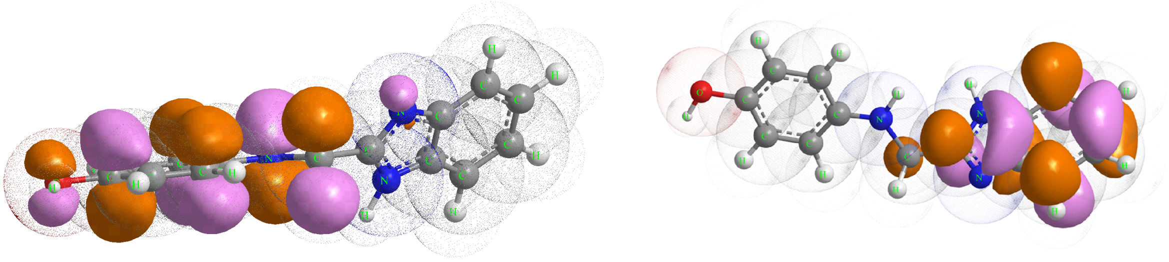

HOMO of BzIm

LUMO of BzIm

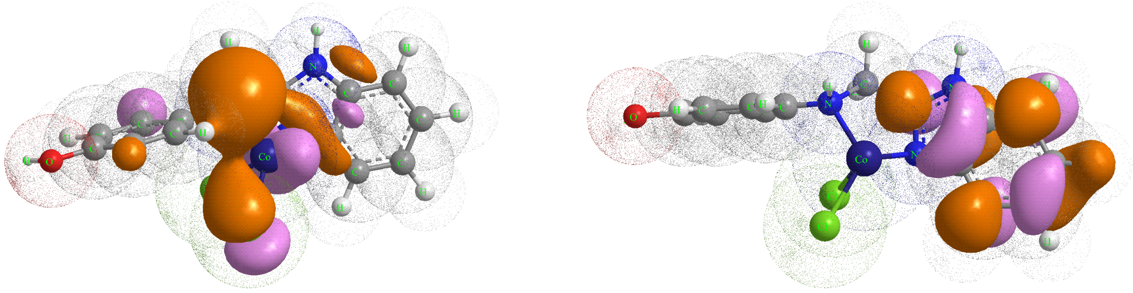

HOMO of $[Co(BzIm)Cl_2]$ (**1**) complex

LUMO of $[Co(BzIm)Cl_2]$ (**1**) complex

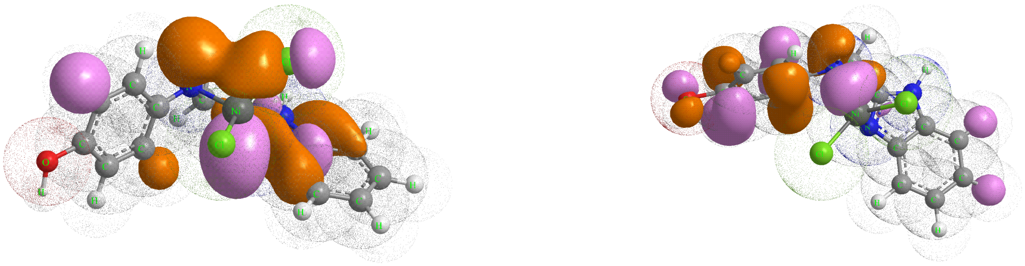

HOMO of $[Ni(BzIm)Cl_2]$ (**2**) complex

LUMO of $[Ni(BzIm)Cl_2]$ (**2**) complex

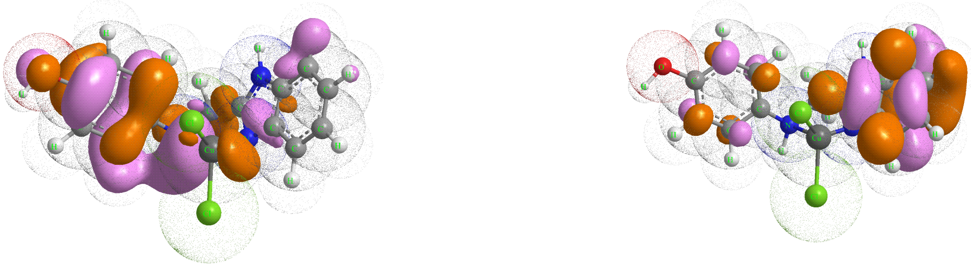

HOMO of $[Cu(BzIm)Cl_2]$ (**3**) complex

LUMO of $[Cu(BzIm)Cl_2]$ (**3**) complex

HOMO of $[Zn(BzIm)Cl_2]$ (**4**) complex

LUMO of $[Zn(BzIm)Cl_2]$ (**4**) complex

Figure 4. HOMO and LUMO orbitals of the ligand (BzIm) and its complexes **1-4**.

Table 1. Weight loss (%), soluble fraction (%), gel content (%) and intrinsic viscosity (g) measurements for rigid PVC in presence of metal complexes acting as photo-stabilizers compared to the reference stabilizer Tinuvin P.

Material	**Weight loss (%)**	**Gel Content (%)**	**Soluble Fraction (%)**
PVC (2 h)	3.3	13.2	86.6
PVC (4 h)	4.7	17.6	82.1
PVC (6 h)	5.3	21	78.6
PVC (8 h)	6.4	26	73.7
PVC + Tp (2 h)	0.4	3.8	95.1
PVC + Tp (4 h)	1	7.1	92.7
PVC + Tp (6 h)	1.6	10.7	89.1
PVC + Tp (8 h)	3	13.7	86
PVC + [Co(BzIm)Cl_2] (**1**) (2h)	1.5	7.6	92.2
PVC + [Co(BzIm)Cl_2] (**1**) (4h)	2.2	11.2	88.6
PVC + [Co(BzIm)Cl_2] (**1**) (6h)	2.8	14.5	85.2
PVC + [Co(BzIm)Cl_2] (**1**) (8h)	4	19.4	80.3
PVC + [Ni(BzIm)Cl_2] **(2)** (2h)	0.9	4.8	94.7
PVC + [Ni(BzIm)Cl_2] **(2)** (4h)	1.3	8.4	90.6
PVC + [Ni(BzIm)Cl_2] **(2)** (6h)	2	11.9	87.6
PVC + [Ni(BzIm)Cl_2] **(2)** (8h)	3.2	15.5	83.9
PVC + [Cu(BzIm)Cl_2] (**3**) (2h)	1.2	6.2	93.7
PVC + [Cu(BzIm)Cl_2] (**3**) (4h)	1.9	9.6	90.2
PVC + [Cu(BzIm)Cl_2] (**3**) (6h)	2.5	13.3	86.6
PVC + [Cu(BzIm)Cl_2] (**3**) (8h)	3.6	17.5	82.2
PVC + [Zn(BzIm)Cl_2] **(4)** (2h)	0.4	3.2	96.1
PVC + [Zn(BzIm)Cl_2] **(4)** (4h)	0.8	6	93.7
PVC + [Zn(BzIm)Cl_2] **(4)** (6h)	1.4	8.3	91.45
PVC + [Zn(BzIm)Cl_2] **(4)** (8h)	2.6	13	88.5

Table 2. Extent of discoloration of photodegraded films of rigid PVC, in presence of 2 wt % of the investigated stabilizers as a function of irradiation time

Material	**Irradiation time (h)**				
	0 h	2 h	4 h	6h	8 h
PVC (blank)	Colorless	Light brown	Light brown	Brown	Dark brown
PVC + Tp	Colorless	Colorless	Light yellow	Light yellow	yellow
PVC + [Co(BzIm)Cl_2] (**1**)	Colorless	Light yellow	Yellow	Dark yellow	Dark yellow
PVC+ [Ni(BzIm)Cl_2] (**2**)	yellow	Light yellow	Light yellow	Light yellow	Yellow
PVC+ [Cu(BzIm)Cl_2] (**3**)	Colorless	Light yellow	Light yellow	Light yellow	Dark yellow
PVC + [Zn(BzIm)Cl_2] (4)	Colorless	Colorless	Light yellow	Light yellow	Light yellow

Table 3. The values of E_{HOMO}, E_{LUMO} and ΔE (LUMO–HOMO) of the ligand and its complexes 1-4, along with energy gaps

Compounds	**E (eV)**		
	$\mathbf{E_{HOMO}}$	$\mathbf{E_{HOMO}}$	$\mathbf{\Delta E = E_{LUMO} - E_{HOMO}}$
BzIm	-5.548	-2.697	2.851
[Co(BzIm)Cl_2] (**1**)	-3.317	-1.882	1.435
[Ni(BzIm)Cl_2] (**2**)	-3.229	-2.052	1.177
[Cu(BzIm)Cl_2] (**3**)	-3.222	-2.026	1.196
[Zn(BzIm)Cl_2] (**4**)	-3.323	-2.161	1.162

Chemical descriptors such as electronic chemical potential (μ) [45], electronegativity (χ) [45, 46], chemical hardness (η), softness (σ) [47], electrophilicity (ω), electron acceptor power (ω+), and electron donor power (ω^-) [46], ionization potential (IP), and electron affinity (EA) [48] are thought to play a significant role in predicting a compound's antiradical power. Table 4 lists the ligands and their complexes' reactivity indices.

Table 4. Reactivity indices of the ligand and its complexes **1-4**.

Compound	**Reactivity indices (eV)**							
	IP[a]	**EA**[b]	**μ**[c]	**η**[d]	**σ**[e]	**ω**[f]	$\boldsymbol{\omega^{+}}$[g]	$\boldsymbol{\omega^{-}}$[h]
BzIm	5.548	2.697	4.122	1.4255	0.701	11.922	0.298	0.423
[Co(BzIm)Cl_2] (**1**)	3.317	1.882	2.599	0.7175	1.393	9.417	0.390	0.515
[Ni(BzIm)Cl_2] (**2**)	3.229	2.052	2.640	0.5885	1.699	11.847	0.498	0.623
[Cu(BzIm)Cl_2] (**3**)	3.222	2.026	2.624	0.598	1.672	11.514	0.485	0.610
[Zn(BzIm)Cl_2] (**4**)	3.323	2.161	2.742	0.581	1.721	12.940	0.527	0.652

[a] IP (eV) = - E_{HOMO}; [b] EA (eV) = - E_{LUMO}; [c] $\mu = \frac{(IP+EA)}{2}$; [d] $\eta = \frac{(IP-EA)}{2}$; [e] $\sigma = \frac{1}{\eta}$; [f] $\omega = \frac{\mu^2}{2\eta}$; [g] $^{+}(Electron\ acceptor\ power) = \frac{(I+3A)^2}{16(I-A)}$; [h] $^{-}(electron\ donor\ power) = \frac{(3I+A)^2}{16(I-A)}$.

It is clear that among all complexes, [Zn(BzIm)Cl_2] (**4**) complex has the lowest value of η, i.e., 0.581eV, whereas [Co(BzIm)Cl_2] (**1**) complex has the highest value (0. 0.653 eV). These findings are consistent with the LUMO-HOMO band gaps of all compounds. Zn(II) complex (**2**) has the highest electronic chemical potential (μ) value (2.742 eV), while Co(II) complex has the lowest chemical potential value (2.599 eV). The results indicate that [Zn(BzIm)Cl_2] (**4**) complex has the lowest electrophilicity index value and is nucleophilic in nature, whereas [Co(BzIm)Cl_2] (**1**) complex has the highest value ω, i.e., 12.940 eV, and is strongly electrophilic in nature. In addition, among the set of complexes, [Zn(BzIm)Cl_2] (**4**) complex has the highest electron acceptor power (ω+) and electron donor power (ω^-) values (0.527eV and 0.652 eV, respectively), while [Co(BzIm)Cl_2] (**1**) complex has the lowest electron acceptor power and electron donor power values (0.390 eV and 0.515 eV, respectively). The theoretical data are consistent with those obtained from experimental data (weight loss %) and the reactivity of complexes follows the order: [Zn(BzIm)Cl_2] (**4**) complex > [Ni(BzIm)Cl_2] (**2**) complex > [Cu(BzIm)Cl_2] (**3**) complex > [Co(BzIm)Cl_2] (**1**) complex.

.

4. Conclusion

Studies of Co^{II}, Ni^{II}, Cu^{II}, and Zn^{II} complexes of Phenyl benzimidazole (BzIm) which is structural commercial, industrial UV-stabilizer for PVC resin have been performed both experimentally and theoretically. The structure of the BzIm complexes was confirmed by the IR, UV-Vis, magnetic, molar conductance, ^{1}H-NMR, MS, XRD and elemental analysis. The central metal(II) ion (Co^{II}, Ni^{II}, Cu^{II}, and Zn^{II}) is coordinated by the pyridine-type nitrogen of benzimidazole ring, secondary amino group and two Cl-ions, forming a distorted square planar geometry. The reaction between BzIm ligand and metal(II) ion, (Co^{II}, Ni^{II}, Cu^{II}, and Zn^{II}) was found to be stoichiometric with the formation of a 1:1 complex. A theoretical DFT/UB3LYP method combined with LANL2DZ basis set shows that all the metal-ligand bonds are of the L→M type. Investigation of the studied compounds as photo-stabilizers for PVC composites has been also explored. The results revealed that the low extent of weight loss, gelation formation, and development of the soluble fraction of the photo-degraded PVC stabilized by metal complexes comparing by the reference UV-absorber. The stabilizing efficiency of the investigated compounds was found to be in the following order: [Zn(BzIm)Cl_2] (**4**) > Tinuvin P (**TP**) > [Ni(BzIm)Cl_2] (**2**) > [Cu(BzIm)Cl_2] (**3**) > [Co(BzIm)Cl_2] (**1**). The stabilizing efficiency of these derivatives is attributes to their radical trapping potency which intervenes with the radical degradation process of PVC

Conflicts of interest

"There are no conflicts to declare".

References:

1. Saeki, Y.; Emura, T. Technical progresses for PVC production. *Progress in Polymer Science*, **2002,** *27* (10), 2055-2131
2. Lima, R.; Silva, J.; Vasconcelos, M. .; Castor, C. A.; Pinto, J. Bibliometric survey of the PVC production-Part I: the continuous polymerization challenge. *Polímeros*, **2023,** *33* (2), e20230013.
3. Mušič, B.; Sever Škapin, A. J. P. Degradation and Stabilization of Polymer Materials. *Polymers*, **2023** (*15*), 1-7.
4. Guillet, J. *Polymer Photophysics and Photochemistry*. Cambridge: Cambridge University Press, **1987**.
5. Marturano, V. Cerruti, P. Ambogi, V., *Polymer additives*. In book: *Polymer Engineering*, **2017,** *2* (6), 20160130.
6. Revanasiddappa, H. D.; Novel Benzimidazole Derived Imine-Based Ligand and its Co (III), Ni (II), Cu (II) and Pt (II) Complexes: Chemical Synthesis, Structure, Antimicrobial, DNA Interaction Studies and Nuclease Activity. *Pharmaceuticals*, **2020**. *16*(1), 125
7. Alvarez, G. A.; Mejıa, E. J. P. Fundamentals, P. o. C. C. Applications, Coordination complexes of copper, silver, and gold. *in book: Photochemistry and Photophysics of Coordination Compounds* **2023**, (293-340).
8. Shobana, S.; Dharmaraja, J.; Selvaraj, S. Mixed ligand complexation of some transition metal ions in solution and solid state: Spectral characterization, antimicrobial, antioxidant, DNA cleavage activities and molecular modeling. *Spectrochimica Acta Part A: Molecular and Biomolecular Spectroscopy* **2013,** *107*, 117-132
9. Yao, H.-C.; Li, M.-M.; Yang, G.-S.; Li, Z.-J.; Zhu, Y., Ketonization of methylene of bis (benzimidazol-2-yl) methane by molecular oxygen under the catalysis of cobalt (II) ion. *Inorganica Chimica Acta*, **2007,** *360* (14), 3959-3964.
10. Ghani, N. T. A.; Mansour, A. M. Palladium (II) and platinum (II) complexes containing benzimidazole ligands: Molecular structures, vibrational frequencies and cytotoxicity. *Journal of Molecular Structure,* **2011,** *991* (1-3), 108-126.
11. Ghani, N. T. A.; Mansour, A. M. Novel palladium (II) and platinum (II) complexes with 1H-benzimidazol-2-ylmethyl-N-(4-bromo-phenyl)-amine: Structural studies and anticancer activity. *European Journal of Medicinal Chemistry*, **2012,** *47*, 399-411.
12. Ryokichi, T.; Seiji, J.; Akira, U.; Eishin, K. J. Derivatographic Studies on Transition Metal Complexes. X. Thermal Octahedral-to-Square Planar Transformation of Ni (NN-deen) 2X2· nH_2O in Solid Phase. *Bulletin of the Chemical Society of Japan (BCSJ),* **1973,** *46* (5), 1454-1456.
13. Mazlan, N. A. Synthesis, Characterization and Biological Activities of Tridentate Ons Schiff Bases and Their Mixed-ligand Metal Complexes Containing Imidazole Or Benzimidazole. *Universiti Putra Malaysia Institutional Repository*, 2014.
14. Rumyantsev, E.; Makarova, S.; Antina, E. J., Protonation and solvation effects in the reaction of zinc 1, 2, 3, 7, 8, 12, 13, 17, 18, 19-Decamethylbiladien-a, c complex formation. *Russian Journal of General Chemistry*, **2009,** *79* (11), 2420-2424.
15. Manjuraj, T.; Krishnamurthy, G.; Bodke, Y. D.; Naik, H. B.; Kumar, H. A. Synthesis, XRD, thermal, spectroscopic studies and biological evaluation of Co (II), Ni (II) Cu (II) metal complexes derived from 2-benzimidazole. *Journal of Molecular Structure*, **2018,** *1171*, 481-487.
16. He, X.; Long, L.; Wu, F.; Le, X.; Chen, X.; Ji, L.; Zhou, Z.., The ternary metal mixed ligand complexes formed by benzimidazole and N, N-bis (2-hydroxyethyl) glycine. *Science in China Series B: Chemistry*, **1999,** *42* (2), 185-194
17. Mangel, D. N. The development of hexaphyrin-expanded porphyrins and deferasirox derivatives for their applications toward f-element coordination. PhD thesis, repositories.lib.utexas.edu, 2022.
18. Raducka, A.; Świątkowski, M.; Korona-Głowniak, I.; Kaproń, B.; Plech, T.; Szczesio, M.; Gobis, K.; Szynkowska-Jóźwik, M. I.; Czylkowska, A. Zinc coordination compounds with benzimidazole derivatives: Synthesis, structure, antimicrobial activity and potential anticancer application. *International Journal of Molecular Sciences* , **2022,** *23* (12), 6595.
19. Raducka, A.; Swiatkowski, M.; Korona-Głowniak, I. Design, Synthesis, and Characterization of Novel Coordination Compounds of Benzimidazole Derivatives with Cadmium. *Pharmaceutics*, **2022**,14(8),1626.
20. Charisiadis, P.; Kontogianni, V. G.; Tsiafoulis, C. G.; Tzakos, A. G.; Siskos, M.; Gerothanassis, I. P. ^{1}H-NMR as a Structural and Analytical Tool of Intra- and Intermolecular Hydrogen Bonds of Phenol-Containing Natural Products and Model Compounds. *Molecules,* **2014,** *19*(9), 13643-13682.
21. Frisch, M.; Trucks, G.; Schlegel, H. B.; Scuseria, G. E.; Robb, M. A.; Cheeseman, J. R.; Scalmani, G.; Barone, V.; Mennucci, B.; Petersson, G. J. I., Wallingford CT, gaussian 09, Gaussian. **2009,** *121*, 150-166.
22. Issa, R. M.; Hassanein, A. A.; El-Mehasseb, I. M.; El-Wadoud, R. I. UV–vis, IR and 1H NMR spectroscopic studies of some 6-chloro, 2-pyridyl hydrazones. *Spectrochimica Acta Part A: Molecular and Biomolecular Spectroscopy,* **2006,** *65* (1), 206-214.
23. Araya-Hernández, C. G.; Morales, R. G.. Chemistry, P. A., Sulfur aromatic heterocycles: A new kind of solar ultraviolet-B radiation actinometers. *Journal of Photochemistry and Photobiology A: Chemistry,* . **2006,** *177* (2-3), 125-128.
24. Issa, R. M.; El-Daly, S. A.; El-Wakiel, N. A. Spectroscopy, B., UV/Vis, IR and 1H NMR spectroscopic studies of bisazo-dianil compounds based on 5-(2-carboxyphenyl azo)-salicylaldehyde and primary diamines. *Spectrochimica Acta Part A: Molecular and Biomolecular Spectroscopy*, **2003,** *59* (4), 723-728.
25. Mazlan, N. A.; Ravoof, T. B. S.; Tiekink, E. R.; Tahir, M. I. M.; Veerakumarasivam, A.; Crouse, K. A. J. Mixed-ligand metal complexes containing an ONS Schiff base and imidazole/benzimidazole ligands: synthesis, characterization, crystallography and biological activity. *Transition Metal Chemistry*, . **2014,** *39*, 633-639.
26. Maru, M. S.; Shah, M. K. J. Synthesis, Characterization and Antimicrobial Evaluation of Transition Metal Complexes of Monodentate 2-(Substituted Phenyl)-1H-benzo [d] imidazoles. Chiang Mai Journal of Science, **2015,** *42* (1), 216-227.

---

27. Bolos, C.; Papazisis, K.; Kortsaris, A.; Voyatzi, S.; Zambouli, D.; Kyriakidis, D. JAntiproliferative activity of mixed-ligand dien-Cu (II) complexes with thiazole, thiazoline and imidazole derivatives. *Journal of Inorganic Biochemistry*, **2002,** *88* (1), 25-36; (
28. Reyes-López, O.; Sánchez-Ruiz, S. A.; Flores-Parra, A.; Leyva, M. A.; Alvarez-Méndez, R. J.; Vela, A.; Rosales-Hoz, M. J. Reactivity of [H2Os3 (CO) 10] with six-membered heterocycles containing sulfur and/or nitrogen atoms. Cleavage of C–S, C–N and C–H bonds to yield linked clusters with S–C, and S–C–N bridging fragments. *Journal of Organometallic Chemistry,* **2014,** *772*, 248-257.
29. Parker, S. F.; Williams, K. P.; Smith, T.; Ramirez-Cuesta, A. J.; Daemen, L. L. Vibrational Spectroscopy of Hexahalo Complexes. *Inorganic Chemistry*, **2022,** *61* (15), 5844-5854.
30. Hoffmann, G. G., *Infrared and Raman Spectroscopy: Principles and Applications*. Walter de Gruyter GmbH & Co KG: 2023.
31. Buttrus, N.; Mohamed, S. J. Synthesis and Characterization of Ni, Cu and Zn complexes with Benzoxazole-2-thionate, Diphenyl Phosphinomethane and Iodine. *Research Journal of Chemical Sciences*, **2013,** *Vol. 3(6), 54-59.*
32. Sultana, S.; Akramullazi, A.; Hossen, M. F.; Asraf, M. A.; Kudrat-E-Zahan, M. J. Transition metal (II) complexes of 2-(2, 5-dimethoxy-benzylidene) hydrazine-1-carbothioamide: synthesis, characterization and their biological evaluation. *Mediterranean Journal of Chemistry,* **2024,** *14* (2), 122-132.
33. Gumus, F.; Eren, G. k. e.; Açık, L.; Celebi, A.; Ozturk, F.; Yılmaz, S. u. k.; Sagkan, R. I.; Gur, S.; Ozkul, A.; Elmalı, A. J. Synthesis, cytotoxicity, and DNA interactions of new cisplatin analogues containing substituted benzimidazole ligands. *Journal of Medicinal Chemistry*, **2009,** *52* (5), 1345-1357.
34. Satyanarayana, S.; Nagasundara, K. Synthesis and Spectral Properties of the Complexes of Cobalt (II), Nickel (II), Copper (II), Zinc (II), and Cadmium (II) with 2-(Thiomethyl-2′-benzimidazolyl)-benzimidazole. *Synthesis and Reactivity in Inorganic and Metal-Organic Chemistry,* **2004,** *34* (5), 883-895.
35. Nakamoto, K., *Infrared and Raman spectra of inorganic and coordination compounds, part B: applications in coordination, organometallic, and bioinorganic chemistry*. John Wiley & Sons: 2009.
36. Nawrocka, W.; Sztuba, B.; Kowalska, M. W.; Liszkiewicz, H.; Wietrzyk, J.; Nasulewicz, A.; Pełczyńska, M.; Opolski, A. J. I. Synthesis and antiproliferative activity in vitro of 2-aminobenzimidazole derivatives. *Farmaco*, **2004,** *59* (2), 83-91.
37. Tosik, A.; Sieron, L.; Bukowska-Strzyzewska, M. J. Catena-Poly [aqua (benzimidazole-N3) copper (II)-μ-malonato-O, O'': O']. *Acta Crystallographica Section C: Structural Chemistry,* **1995,** *51* (10), 1987-1989.
38. Fnfoon, D. Y.; Al-Adilee, K. J. J. Synthesis and spectral characterization of some metal complexes with new heterocyclic azo imidazole dye ligand and study biological activity as anticancer. *Journal of Molecular Structure*, **2023,** *1271*, 134089.
39. Xu, L. Y.; Chai, Y. M.; Li, C. G.; Chai, L. Q.., Co (II) and Cd (II) complexes with imidazole-2-carboxaldehyde groups: spectroscopic, antibacterial, Hirshfeld surfaces analyses, and TD/DFT calculations. *Applied Organometallic Chemistry*, **2021,** *35* (8), e6279.
40. Kolhe, N. H.; Jadhav, S. S.; Thube, D. R.; Takate, S. J.; Bankar, A. V.; Moharekar, S. T.; Pawar, H. R.; Moharekar, S. S. J. New Mn (II), Co (II), Ni (II) and Cu (II) homoleptic complexes with 6-chloro-5-7-dimethyl-4oxo-4H-chromene-3-carbaldehydes and its heteroleptic complexes with quinoline-8 ol: synthesis, characterization and antimicrobial activity. *Research on Chemical Intermediates*, **2021,** *47*, 459-481.
41. Larbi, K. S.; Bouchoucha, A.; Bourouai, M. A.; Djebbar, S. J. Novel metal (II) complexes with 2, 2'-bithiophene ligands as promising antibacterial agents: Spectral investigation, electrochemical behavior, DFT studies, in vitro and in silico biological properties. *Journal of Molecular Structure,* **2023,** *1291*, 135901.
42. Karnik, A. V.; Hasan, M., *Stereochemistry: a three-dimensional insight*. Elsevier: 2021.
43. De Abreu, H.A.; Lago, I.A.d.S.; Souza, G.P.; Piló-Veloso, D.; Duarte, H.A.; Alcântara, A.F.d.C. Antioxidant activity of (+)-bergenin—a phytoconstituent isolated from the bark of Sacoglottis uchi Huber (Humireaceae). *Org. Biomol. Chem.* **2008**, 6, 2713–2718
44. Makhlouf, J.; Louis, H.; Benjamin, I.; Amodu, I. O.; Valkonen, A.; Abuelizz, H. A.; Bakri, Y. E.; Al-Salahi, R.; Sta, W. S. J. Preparation of novel [Co (SCN) 4] hybrid material: crystal structure investigation, DFT mechanistic analysis, antioxidant activity, and molecular docking study for potential inflammatory disorder control. *Journal of Sulfur Chemistry,* **2024**, 1-23.
45. Muthu, S.; Renuga, S. J. Molecular orbital studies (hardness, chemical potential, electronegativity and electrophilicity), vibrational spectroscopic investigation and normal coordinate analysis of 5-{1-hydroxy-2-[(propan-2-yl) amino] ethyl} benzene-1, 3-diol. *Spectrochimica Acta Part A: Molecular and Biomolecular Spectroscopy,* **2014,** *118*, 683-694.
46. Zhan, C.-G.; Nichols, J. A.; Dixon, D. A. Ionization potential, electron affinity, electronegativity, hardness, and electron excitation energy: molecular properties from density functional theory orbital energies. *The Journal of Physical Chemistry A,* **2003,** *107* (20), 4184-4195.
47. Kaya, S.; Kaya, C. A new method for calculation of molecular hardness: a theoretical study. *Computational and Theoretical Chemistry*, **2015,** *1060*, 66-70.
48. Mebi, C. A. DFT study on structure, electronic properties, and reactivity of cis-isomers of [(NC 5 H 4-S) 2 $Fe(CO)_2$]. *Journal of Chemical Sciences*, **2011,** *123*, 727-731.